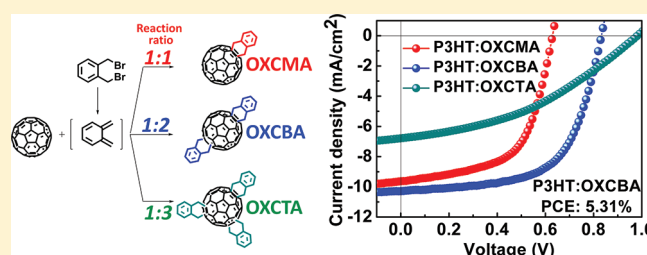


Facile Synthesis of *o*-Xylenyl Fullerene Multiadducts for High Open Circuit Voltage and Efficient Polymer Solar CellsKi-Hyun Kim,[†] Hyunbum Kang,[†] So Yeon Nam,[‡] Jaewook Jung,[‡] Pan Seok Kim,[‡] Chul-Hee Cho,[†] Changjin Lee,[‡] Sung Cheol Yoon,^{*,‡} and Bumjoon J. Kim^{*,†}[†]Department of Chemical and Biomolecular Engineering, Korea Advanced Institute of Science and Technology (KAIST), Daejeon 305-701, Korea[‡]Advanced Materials Division, Korea Research Institute of Chemical Technology, Daejeon 305-600, Korea

Supporting Information

ABSTRACT: The ability to control the lowest unoccupied molecular orbital (LUMO) level of an electron-accepting material is a critical parameter for producing highly efficient polymer solar cells (PSCs). Soluble bis-adducts of C₆₀ have great potential for improving the V_{OC} in PSCs because of their high LUMO level. In this work, we have developed a novel *o*-xylenyl C₆₀ bis-adduct (OXCBA) via a [4 + 2] cycloaddition between C₆₀ and an irreversible diene intermediate from α,α' -dibromo-*o*-xylene. OXCBA was successfully applied as the electron acceptor with poly(3-hexylthiophene) (P3HT) in a PSC, showing a high efficiency of 5.31% with V_{OC} of 0.83 V. This composite showed a nearly 50% enhancement in efficiency compared to the P3HT:PCBM control device (3.68% with V_{OC} of 0.59 V). Furthermore, tuning the molar ratio between C₆₀ and the α,α' -dibromo-*o*-xylene group from 1:1 to 1:3 in the reaction scheme enables facile control over the number of *o*-xylenyl solubilizing groups ultimately tethered to the fullerene, thus producing *o*-xylenyl C₆₀ mono-, bis-, and tris-adducts (OXCMA, OXCBA, and OXCTA) with different LUMO levels. As the number of solubilizing groups increased, V_{OC} values of the P3HT-based BHJ solar cells increased from 0.63 V (OXCMA) to 0.83 V (OXCBA) to 0.98 V (OXCTA). This series of *o*-xylenyl C₆₀ multiadducts provides a model system for investigating the molecular structure-device function relationship, especially with respect to changes in the number of solubilizing groups on the electron acceptor.

KEYWORDS: electron acceptors, bisadduct fullerene, high open circuit voltage, polymer solar cells



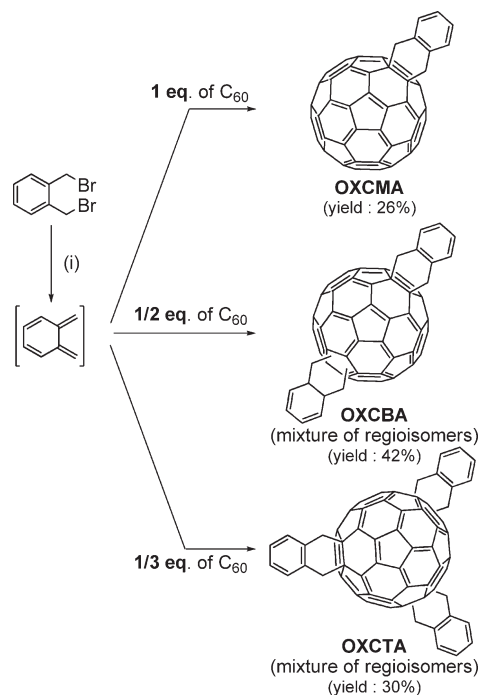
INTRODUCTION

Polymer solar cells (PSCs) are a promising alternative for clean and sustainable energy due to their simple fabrication, mechanical flexibility, and potential for a low-cost, large-scale manufacturing scheme.^{1–4} To date, the combination of poly(3-hexylthiophene) (P3HT) as the electron donor and [6,6]-phenyl-C₆₁-butyric acid methyl ester (PCBM) as the electron acceptor represents one of the most promising candidates for the active layer in bulk heterojunction (BHJ) type PSCs, showing a relatively high power conversion efficiency (PCE) of more than 4%.^{5,6} Low-bandgap conjugated polymers have also been studied intensively in recent years with the aim of matching a greater part of the solar spectrum in their absorption spectra and hence harvesting more photon flux; these polymers produce high efficiencies of more than 6–7%.^{7–13} However, many of the reported conjugated polymers, including P3HT, suffer from low efficiency in photovoltaics due to loss of V_{OC}.^{14–16} Because V_{OC} is proportional to the difference between the lowest unoccupied molecular orbital (LUMO) level of the acceptor and the highest occupied molecular orbital (HOMO) level of the donor material,¹⁷ the use of PCBM with a relatively low-lying LUMO level limits the V_{OC} of the PSCs.

To address this problem, researchers have recently designed and synthesized a number of fullerene derivatives with high LUMO levels for use as electron acceptors in high V_{OC} PSCs.^{18–22} Among these electron acceptors based on fullerene, fullerene bis-adducts, which have two solubilizing groups, effectively increase V_{OC} compared with P3HT:PCBM blended systems. The fullerene bis-adducts have higher LUMO energy levels because of the reduction of the molecule's electron affinity due to the presence of fewer unsaturated bonds as compared with fullerene monoadducts. Blom et al. reported bis-PCBM (a regioisomeric bis-adduct of PCBM) used as an electron acceptor for PSCs.¹⁸ The V_{OC} of the P3HT:bis-PCBM BHJ solar cells was 0.15 V higher than that of P3HT:PCBM because of the ~0.1 eV higher LUMO energy level of bis-PCBM as compared to PCBM. Recently, Laird²³ and Li et al.^{24–26} reported a remarkable bis-adduct fullerene derivative, indene-C₆₀ bis-adduct (ICBA). Through the Diels–Alder reaction of indene with the C₆₀, ICBA achieves a LUMO energy level that is 0.17 eV higher than that of singly functionalized PCBM. A PSC consisting of P3HT and ICBA demonstrated a V_{OC} of 0.84 V and a

Received: September 14, 2011

Published: October 24, 2011

Scheme 1. Synthetic Route to *o*-Xylenyl C₆₀ Multi adducts^a

^a (i) KI, 18-crown-6, *o*-DCB, reflux, 48 h.

PCE of 5.44%, whereas a cell based on P3HT:PCBM displayed a V_{OC} of 0.58 V and a PCE of 3.88% under the same experimental conditions.²⁴

Although the use of ICBA in P3HT solar cells induced a remarkable increase in the V_{OC} and PCE, the synthesis of ICBA requires the improvement for large-scale synthesis due to the following reasons: First, a large excess of indene (mole ratio of indene to C₆₀ = 20:1) is required to produce ICBA, due to the reversible formation of its diene form during the reaction. In addition, because of the presence of excess amounts of indene, controlling the number of indene groups attached to the fullerene is difficult and thus the synthesis of ICBA is accompanied by formation of the monoadduct and tris-adduct indene fullerenes as byproducts, requiring a multistep purification procedure. Finally, indene and indene-derivatives are relatively expensive.

Herein, we report a new fullerene-based electron acceptor, *o*-xylenyl C₆₀ bis-adduct (OXCBA), using α,α' -dibromo-*o*-xylene as a building block. Because the diene intermediate (*o*-xylylene) of α,α' -dibromo-*o*-xylene forms irreversibly in the dark,²⁷ the OXCBA molecule can be synthesized using an exact ratio of α,α' -dibromo-*o*-xylene to fullerene (2:1) with formation of a minimal amount of byproducts. Due to the excellent reaction control, simple tuning of the molar ratio between C₆₀ and α,α' -dibromo-*o*-xylene group from 1:1 to 1:3 in the reaction enables facile control over the number of *o*-xylenyl solubilizing groups in final fullerene product, thus producing the *o*-xylenyl C₆₀ mono-, bis-, and tris-adducts (OXCMA, OXCBA, and OXCTA), each having a different LUMO energy. *o*-Xylenyl C₆₀ multiadducts were successfully applied as the electron acceptor with poly(3-hexylthiophene) (P3HT) in a PSC, with the finished devices showing that the progressive addition of solubilizing groups to the fullerene results in significant increases in their LUMO level and thus V_{OC} (OXCMA, 0.63 V; OXCBA, 0.83 V; and OXCTA, 0.98 V). In particular, the P3HT/OXCBA device

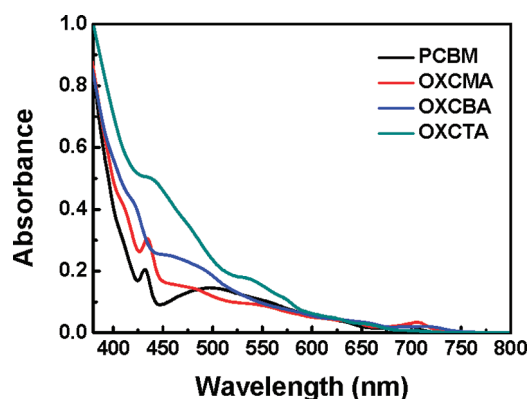


Figure 1. UV-vis absorption spectra of PCBM (black line), OXCMA (red line), OXCBA (blue line), and OXCTA (green line) solution ($8 \times 10^{-5} \text{ mol L}^{-1}$) in *o*-DCB.

showed the highest efficiency of 5.31% with V_{OC} of 0.83 V, which is nearly 50% higher than the P3HT:PCBM control device (3.68% with V_{OC} of 0.59 V).

RESULTS AND DISCUSSION

o-Xylenyl C₆₀ multiadducts were synthesized using a Diels–Alder reaction ([4 + 2] cycloaddition) between fullerene and the diene intermediate from α,α' -dibromo-*o*-xylene. (Scheme 1; see the Supporting Information for details) It is known that the solubilizing groups could be effectively attached to fullerene by using α,α' -dibromo-*o*-xylene derivatives as diene precursor.^{28,29} By using 1.0, 2.0, and 3.0 equivalent of α,α' -dibromo-*o*-xylene to C₆₀, the crude products contained OXCMA, OXCBA, and OXCTA as the major products, respectively. After purifying by flash silica column chromatography (hexane/toluene eluent gradient system), the synthesized *o*-xylenyl C₆₀ multiadducts were confirmed through ¹H NMR spectroscopy, MALDI-TOF mass spectrometry, and elemental analysis (see Figures S1–S3 in the Supporting Information). The thermal properties of *o*-xylenyl C₆₀ multiadducts were measured by thermal gravimetric analysis (TGA), showing high thermal stability (see Figure S4 in the Supporting Information). The onset points of weight loss of OXCMA, OXCBA, and OXCTA were above 400 °C, which are similar to that of PCBM. The weight loss of *o*-xylenyl C₆₀ multiadducts at 600 °C was lower than 10% and increased with an increase in the number of solubilizing groups in order of OXCMA, OXCBA, and OXCTA. From differential scanning calorimetry (DSC) measurement, OXCMA showed higher melting point of 345 °C than that of PCBM (~285 °C) (Figure S5). In contrast, under the same measurement condition, no melting transition was observed for OXCBA and OXCTA including larger number of solubilizing groups. We suggest that OXCBA and OXCTA show weaker crystalline behaviors because of the presence of multisolubilizing groups added to C₆₀ that prevent close packing between spherical C₆₀.³⁰

The light absorption ability of electron acceptors is of great importance in determining their potential contribution to J_{SC} in PSCs. The absorption spectra of PCBM, OXCMA, OXCBA, and OXCTA solutions ($8 \times 10^{-5} \text{ mol L}^{-1}$) in *o*-dichlorobenzene, in the visible region (380–800 nm) are shown in Figure 1. Interestingly, *o*-xylenyl C₆₀ multiadducts absorb more visible light between 400 and 500 nm than does PCBM at the same concentration. Furthermore, as the number of solubilizing groups in the fullerene increases, the light absorption intensity in the visible region also

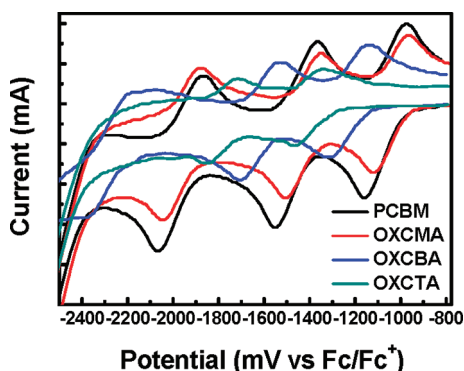


Figure 2. Cyclic voltammograms of PCBM (black line), OXCMA (red line), OXCBA (blue line), and OXCTA (green line) in *o*-DCB with 0.1 M [NBu⁴][BF⁴] at 10 mV s⁻¹.

Table 1. Electrochemical Properties of PCBM, OXCMA, OXCBA, and OXCTA

electron acceptors	E_1 (V)	E_2 (V)	$E_{\text{red}}^{\text{on}}$ (V)	LUMO (eV)
PCBM	-1.14	-1.54	-0.97	-3.83
OXC ₆₀ MA	-1.12	-1.51	-0.97	-3.83
OXC ₆₀ BA	-1.33	-1.72	-1.14	-3.66
OXC ₆₀ TA	-1.47	-1.85	-1.30	-3.50

increases. From these results, higher values of J_{SC} in the PSCs are expected to result from the use of *o*-xylenyl C₆₀ multiadducts with a greater number of solubilizing groups.

The LUMO/HOMO levels of fullerene derivatives are among the most important factors that determine the potential of these compounds as electron acceptors in photovoltaic cells. The electrochemical properties of PCBM, OXCMA, OXCBA, and OXCTA were therefore carefully measured using cyclic voltammetry (CV). The CV curves of the four different electron acceptor materials are shown in Figure 2, and the electrochemical properties of these materials are summarized in Table 1. PCBM, OXCMA, and OXCBA exhibit three quasi-reversible reduction waves in the negative potential range from 0 to -2.5 V. On the other hand, OXCTA shows two quasi-reversible reduction waves in the same range, as reducing the number of sp² carbons in fullerene results in a loss of reversibility for one of the one-electron reduction events.³¹ In the case of OXCMA, the first (E_1) and second (E_2) reduction potentials are almost identical to those of PCBM. In contrast, the E_1 and E_2 of OXCBA and OXCTA are negatively shifted by about 0.21 and 0.34 V, respectively, relative to OXCMA.

The LUMO energy levels of the fullerene-based electron acceptors were estimated from their onset reduction potentials. The onset reduction potentials ($E_{\text{red}}^{\text{on}}$) of PCBM, OXCMA, OXCBA, and OXCTA are -0.97, -0.97, -1.14, and -1.30 V, respectively, vs Fc/Fc⁺. As shown in Table 1, whereas OXCMA has a LUMO level at the same energy relative to that of PCBM (-3.83 eV), OXCBA has a higher LUMO level by 0.17 eV as compared to the monoadduct fullerenes PCBM and OXCMA. Furthermore, the LUMO level of OXCTA (-3.50 eV) is the highest among the four fullerene-based electron acceptors. The higher LUMO levels of OXCBA and OXCTA are attributed to the presence of the extra solubilizing groups and the resulting decrease in the sp² orbital number (the PCBM and OXCMA have 58 sp² orbitals, whereas the

OXCBA and OXCTA have 56 and 54 sp² orbitals, respectively) and the electron affinity of the fullerene. The higher LUMO energy levels found in OXCBA and OXCTA are desirable because they lead to higher values of V_{OC} in BHJ-type organic solar cell devices.

To elucidate the relationship between the molecular structure of the fullerene derivatives and the performance of solar cell devices, BHJ-type PSCs (ITO/PEDOT:PSS/P3HT:electron acceptor/LiF/Al) were fabricated based on blends of these fullerene derivatives with P3HT, and their performances were measured. Figure 3a shows the current density versus voltage ($J-V$) curves of the devices under AM 1.5 illumination at 100 mW cm⁻². Table 2 summarizes the device characteristics of the P3HT-based BHJ solar cells mixed with PCBM, OXCMA, OXCBA, and OXCTA as electron acceptors. The P3HT:OXCMA device exhibited a peak performance of 3.60% (V_{OC} , 0.63 V; J_{SC} , 9.63 mW cm⁻²; FF, 0.59; and PCE, 3.60%) at a P3HT:OXCMA weight ratio of 1:0.6, and its performance was almost identical to that of the P3HT:PCBM control device (V_{OC} , 0.59 V; J_{SC} , 9.47 mW cm⁻²; FF, 0.66; and PCE, 3.68%) at a P3HT:PCBM weight ratio of 1:0.7. It should be noted that the P3HT:OXCBA device outperformed (V_{OC} , 0.83 V; J_{SC} , 10.3 mW cm⁻²; FF, 0.62; and PCE, 5.31%) the P3HT/monoadduct fullerene (PCBM and OXCMA) devices. The dramatic increase in the PCE of the P3HT:OXCBA device was mainly due to an increase in V_{OC} (its value increased by 0.24 V compared to that of the P3HT:PCBM device), which is caused by the higher LUMO level of the OXCBA molecule. The trend for the increase of V_{OC} and device performance observed in this study is similar to that observed in the related ICBA-based devices reported in the literature.^{25,26} The slightly increased J_{SC} of OXCMA and OXCBA also resulted in an increase in PCE compared with PCBM. These results are well matched with the enhanced light absorption of OXCMA and OXCBA as compared with PCBM in the visible region. Of particular interest is that the use of OXCTA as an electron acceptor produced a further increase in V_{OC} of 0.98 V. To the best of our knowledge, this is the highest V_{OC} reported to date for polythiophene- and fullerene-based BHJ-type PSCs. It is well-known that V_{OC} is mainly determined by the difference between the LUMO level of the electron acceptor and the HOMO level of the electron donor.³² The increase in the LUMO levels of OXCMA, OXCBA and OXCTA (-3.83, -3.66, and -3.50 eV, respectively) results in increasing gaps between the LUMO level of each fullerene derivative and the HOMO level of P3HT, causing an increase in the V_{OC} for the OXCMA, OXCBA, to OXCTA devices. Also, the OXCBA showed remarkable long-term stability during 18 months in encapsulated PSCs at room temperature without illumination. The long-term stability data are summarized in Figure S6 and Table S1 in the Supporting Information.

External quantum efficiencies (EQEs) were measured under optimized device conditions for P3HT:PCBM, OXCMA, OXCBA, and OXCTA, as shown in Figure 3b. Between 400 and 650 nm, the maximum EQEs of P3HT:OXCMA, OXCBA, and OXCTA devices are 55.5, 59.9, and 42.1% at 510 nm, respectively, and 53.1% at 490 nm in the case of P3HT:PCBM. The EQE value of the OXCBA-based device is higher than that for PCBM, which is partly a result of better absorption of the OXCBA molecule as shown in Figure 1. The measured J_{SC} for the four PSC devices are well matched with integrated J_{SC} (P3HT:OXC₆₀MA, 9.36 mA cm⁻²; OXCBA, 10.1 mA cm⁻²; OXCTA, 6.74 mA cm⁻²; and PCBM, 9.31 mA cm⁻²) obtained from the EQE spectrum within a 2% error.

One advantage of this system is that this series of *o*-xylenyl C₆₀ multiadducts provides a model system for investigating the

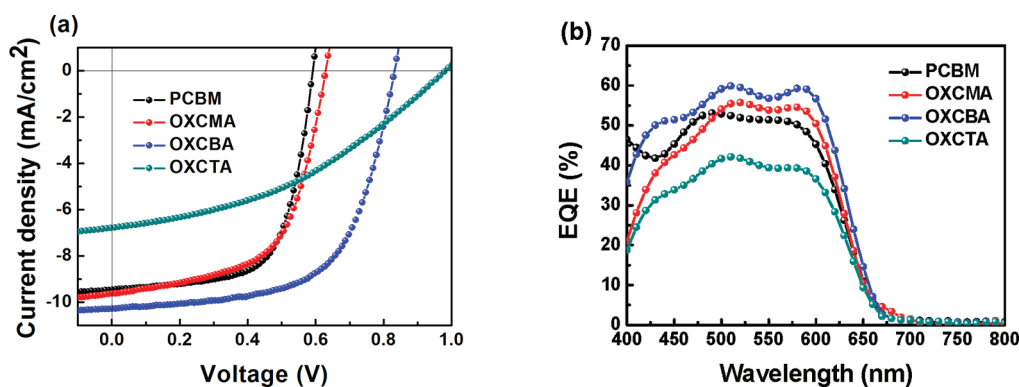


Figure 3. (a) Current density–voltage curves and (b) external quantum efficiencies (EQEs) of OPVs based on P3HT:PCBM (wt ratio = 1:0.7), P3HT:OXCMA (1:0.6), P3HT:OXCBA (1:0.6), and P3HT:OXCTA (1:0.8) BHJ devices under AM 1.5 illumination at 100 mW cm^{-2} .

molecular structure–device function relationship, particularly with regards to the effect of the number of solubilizing groups, on the opto-electronic properties of the fullerene derivatives. The donor/acceptor weight ratio of P3HT:electron acceptor in blended films was carefully tuned, while the concentration of P3HT in the blend solution was fixed to 15 mg/mL to produce the similar film thickness ($\sim 120 \text{ nm}$). Interestingly, the optimum donor:acceptor weight ratio for the device consisting of different fullerene derivative blends with P3HT was varied from 1:0.6 to 1:0.8 as shown in Table 2. It was found that a higher weight ratio of fullerene derivatives was required as the number of solubilizing groups was increased from OXCMA, OXCBA, to OXCTA. This could be explained by the fact that different fullerene derivatives of OXCMA, OXCBA, and OXCTA show a decrease in the weight fraction of the C_{60} molecule, whereas the molecular weight (MW) of OXCMA, OXCBA, and OXCTA increases from 832.8 to 928.5 to 1032.6, respectively. The weight fraction of the C_{60} molecule (F_{C60}) in each P3HT:electron acceptor blend can be calculated from the weight of the C_{60} part (W_{C60}) to the total weight of the P3HT:electron acceptor blend ($W_{P3HT} + W_{\text{acceptor}}$), as in the following equation

$$F_{C60} = \frac{W_{C60}}{(W_{P3HT} + W_{\text{acceptor}})}$$

$$= \frac{W_{\text{acceptor}}}{(W_{P3HT} + W_{\text{acceptor}})} \frac{W_{C60}}{W_{\text{acceptor}}}$$

Therefore, F_{C60} for the best device of P3HT:OXCMA (P3HT:OXCMA, weight ratio = 1:0.6) is calculated to be 0.325. Interestingly, under the best device conditions F_{C60} for P3HT:OXCBA (1:0.65) and P3HT:OXCTA (1:0.8) are found to be very similar (0.306 and 0.310, respectively). This suggests that the amount of C_{60} molecules required for the best device performance is very similar in P3HT:OXCMA, OXCBA, and OXCTA devices used in our study. This trend is consistent with the previous finding in the system of P3HT:bis-PCBM.^{18,20}

To gain insight into the operation of BHJ solar cells, the charge-carrier mobilities of the P3HT:fullerene derivative blends were measured under the best conditions for each device. The space-charge-limited current (SCLC) mobility measures the hole and electron mobility in the direction perpendicular to the electrodes; thus, it is the most representative measurement of charge-carrier mobility for solar cells. To measure the hole and electron mobilities of different fullerene derivative blends with

Table 2. Device Characteristics of Solar Cells Composed of P3HT as Electron Donor and Four Fullerene Electron Acceptors with Various Weight Ratio under AM 1.5 G-Simulated Solar Illumination (100 mW cm^{-2})

active layer (w/w)	V_{OC} (V)	J_{SC} (mA cm^{-2})	FF	PCE (%)
P3HT:PCBM (1:0.6)	0.59	8.95	0.62	3.28
P3HT:PCBM (1:0.7)	0.59	9.47	0.66	3.68
P3HT:PCBM (1:0.8)	0.59	9.07	0.67	3.58
P3HT:OXCMA (1:0.6)	0.63	9.63	0.59	3.60
P3HT:OXCMA (1:0.7)	0.62	9.17	0.59	3.37
P3HT:OXCMA (1:0.8)	0.64	8.93	0.57	3.22
P3HT:OXCBA (1:0.6)	0.83	10.3	0.62	5.31
P3HT:OXCBA (1:0.7)	0.81	10.0	0.64	5.21
P3HT:OXCBA (1:0.8)	0.80	9.18	0.65	4.81
P3HT:OXCTA (1:0.6)	0.95	6.95	0.36	2.37
P3HT:OXCTA (1:0.7)	0.95	6.84	0.38	2.47
P3HT:OXCTA (1:0.8)	0.98	6.79	0.40	2.63

P3HT, the ITO/PEDOT:PSS/blend/Au and ITO/ CS_2CO_3 /blend/LiF/Al devices were fabricated for hole-only and electron-only devices, respectively. Fabrication and J – V curves of hole- and electron-only devices are described in Figure 4. Table 3 summarizes the hole and electron mobilities, as well as the ratio of the hole-to-electron mobilities (μ_h/μ_e) of the devices based on P3HT blended with PCBM, OXCMA, OXCBA, and OXCTA under their optimized best device conditions. While all the devices showed similar hole mobilities ($\sim 3 \times 10^{-4} \text{ cm}^2 \text{ V}^{-1} \text{ s}^{-1}$), there were significant differences in the electron mobilities between the devices. Whereas the electron mobilities of P3HT:PCBM, P3HT:OXCMA, and P3HT:OXCBA showed similar values of approximately $2 \times 10^{-4} \text{ cm}^2 \text{ V}^{-1} \text{ s}^{-1}$, further addition of *o*-xylene solubilizing groups (P3HT:OXCTA) resulted in a lowering of the electron mobility by 2 orders of magnitude. This result is consistent with previous findings for devices using tris-PCBM^{20,33} and likely results from an increase in disorder in the fullerene phase due to the addition of the side chains and the presence of a higher number of isomers possible for the tris-adducts, both of which prevent efficient packing between fullerenes and decrease electron transport through the fullerene phase. The parameter that represents the ratio of the hole-to-electron mobilities (μ_h/μ_e) in the polymer:acceptor blends is crucial to understanding the optoelectronic properties of BHJ

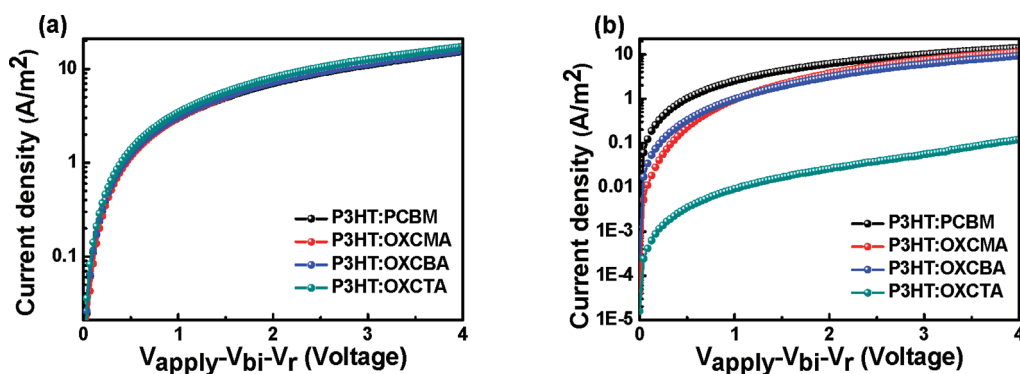


Figure 4. Measured space-charge-limited J - V characteristics of the P3HT:PCBM/OXCMA/OXCBA/OXCTA blend devices under dark conditions using the optimized device condition for (a) hole- and (b) electron-only devices.

Table 3. Calculated Hole and Electron Mobility Values and Electron-Hole Ratio of P3HT:PCBM/OXCMA/OXCBA/OXCTA System at Optimized Condition by SCLC Method

blend system	μ_h ($\text{cm}^2 \text{V}^{-1} \text{s}^{-1}$)	μ_e ($\text{cm}^2 \text{V}^{-1} \text{s}^{-1}$)	μ_h/μ_e
P3HT:PCBM	2.98×10^{-4}	2.31×10^{-4}	1.29
P3HT:OXCMA	3.69×10^{-4}	2.34×10^{-4}	1.58
P3HT:OXCBA	3.08×10^{-4}	2.09×10^{-4}	1.47
P3HT:OXCTA	3.31×10^{-4}	1.00×10^{-6}	331

solar cells, particularly with respect to the fill factor. Whereas P3HT:PCBM, P3HT:OXCMA, and P3HT:OXCBA exhibited relatively well-balanced μ_h/μ_e values, the P3HT:OXCTA device showed an unbalanced ratio of μ_h/μ_e due to its lower electron mobility. It is known that balanced charge-carrier transport is an important factor for increasing the fill factor (FF) in BHJ solar cells.^{34,35} When charge transport in the device is unbalanced, as is found for P3HT:OXCTA, charge accumulation could occur in the device, and the photocurrent could be space-charge-limited. Therefore, the unbalanced μ_h/μ_e value could be one of the reasons for the lower J_{SC} and FF in the P3HT:OXCTA device as compared with the other devices studied here.

CONCLUSIONS

In summary, we successfully synthesized a series of *o*-xylenyl C_{60} multiadducts as novel electron acceptors using α,α' -dibromo-*o*-xylene as a solubilizing group. The number of solubilizing groups was easily controlled by adjusting the molar ratio between C_{60} and the α,α' -dibromo-*o*-xylene group from 1:1 to 1:3 in the synthesis to produce the *o*-xylenyl C_{60} mono-, bis-, and tris-adducts (OXCMA, OXCBA, and OXCTA). We have studied the effect of the number of solubilizing groups attached to the fullerene on the light absorption and electrochemical properties, and have made correlations between the number of solubilizing groups and the parameters for photovoltaic performance, especially V_{OC} . As the LUMO energy level of the *o*-xylenyl C_{60} multiadducts gradually rose from OXCMA (-3.83 eV) to OXCBA (-3.66 eV) to OXCTA (-3.50 eV), the V_{OC} values of the P3HT-based BHJ solar cells also increased from 0.63 V (OXCMA) to 0.83 V (OXCBA) to 0.98 V (OXCTA). To the best of our knowledge, this value is the highest V_{OC} reported to date for polythiophene- and fullerene-based BHJ-type organic solar cell devices. Although the P3HT:OXCTA device showed an extremely high V_{OC} of 0.98 V, the P3HT:OXCBA device showed the best PCE of 5.31%. The

depressed performance of the P3HT:OXCTA cell relative to the P3HT:OXCBA cell was a result of lower J_{SC} and FF due to its unbalanced hole and electron mobilities. From these results, OXCBA has great possibility for replacing PCBM as an electron acceptor for PSCs and may contribute to advancing the commercialization of PSCs.

ASSOCIATED CONTENT

S Supporting Information. Materials and methods, detailed experimental procedures, and additional data (PDF). This material is available free of charge via the Internet at <http://pubs.acs.org>.

AUTHOR INFORMATION

Corresponding Author

*E-mail: bumjoonkim@kaist.ac.kr (B.J.K.); yoonsch@kricr.re.kr (S.C.Y.).

ACKNOWLEDGMENT

This research was supported by the Korea Research Foundation Grant funded by the Korean Government (2009-0081500, 2010-0029611, 2011-0027240), and the Project of the Office of KAIST EEWS Initiative (EEWS-2011-N01110441). The authors thank Drs. Kyung Kon Kim and Claire H. Woo for valuable discussions.

REFERENCES

- (1) Krebs, F. C. *Sol. Energy Mater. Sol. Cells* **2009**, *93*, 394–412.
- (2) Günes, S.; Neugebauer, H.; Sariciftci, N. S. *Chem. Rev.* **2007**, *107*, 1324–1338.
- (3) Arias, A. C.; MacKenzie, J. D.; McCulloch, I.; Rivnay, J.; Salleo, A. *Chem. Rev.* **2010**, *110*, 3–24.
- (4) Brabec, C. J.; Sariciftci, N. S.; Hummelen, J. C. *Adv. Funct. Mater.* **2001**, *11*, 15–26.
- (5) Li, G.; Shrotriya, V.; Huang, J.; Yao, Y.; Moriarty, T.; Emery, K.; Yang, Y. *Nat. Mater.* **2005**, *4*, 864–868.
- (6) Ma, W.; Yang, C.; Gong, X.; Lee, K.; Heeger, A. J. *Adv. Funct. Mater.* **2005**, *15*, 1617–1622.
- (7) Piliago, C.; Holcombe, T. W.; Douglas, J. D.; Woo, C. H.; Beaujuge, P. M.; Fréchet, J. M. J. *J. Am. Chem. Soc.* **2010**, *132*, 7595–7597.
- (8) Chu, T.-Y.; Lu, J.; Beaupré, S.; Zhang, Y.; Pouliot, J.-R. m.; Wakim, S.; Zhou, J.; Leclerc, M.; Li, Z.; Ding, J.; Tao, Y. *J. Am. Chem. Soc.* **2011**, *133*, 4250–4253.

- (9) Price, S. C.; Stuart, A. C.; Yang, L.; Zhou, H.; You, W. *J. Am. Chem. Soc.* **2011**, *133*, 4625–4631.
- (10) Zhou, H.; Yang, L.; Stuart, A. C.; Price, S. C.; Liu, S.; You, W. *Angew. Chem., Int. Ed.* **2011**, *50*, 2995–2998.
- (11) Ong, K.-H.; Lim, S.-L.; Tan, H.-S.; Wong, H.-K.; Li, J.; Ma, Z.; Moh, L. C. H.; Lim, S.-H.; de Mello, J. C.; Chen, Z.-K. *Adv. Mater.* **2011**, *23*, 1409–1413.
- (12) Liang, Y. Y.; Feng, D. Q.; Wu, Y.; Tsai, S. T.; Li, G.; Ray, C.; Yu, L. P. *J. Am. Chem. Soc.* **2009**, *131*, 7792–7799.
- (13) Park, S. H.; Roy, A.; Beaupre, S.; Cho, S.; Coates, N.; Moon, J. S.; Moses, D.; Leclerc, M.; Lee, K.; Heeger, A. J. *Nat. Photonics* **2009**, *3*, 297–U295.
- (14) Moulé, A. J.; Tsami, A.; Bünnagel, T. W.; Forster, M.; Kronenberg, N. M.; Scharber, M.; Koppe, M.; Morana, M.; Brabec, C. J.; Meerholz, K.; Scherf, U. *Chem. Mater.* **2008**, *20*, 4045–4050.
- (15) Zhou, E.; Nakamura, M.; Nishizawa, T.; Zhang, Y.; Wei, Q.; Tajima, K.; Yang, C.; Hashimoto, K. *Macromolecules* **2008**, *41*, 8302–8305.
- (16) Perzon, E.; Zhang, F.; Andersson, M.; Mammo, W.; Inganäs, O. *Adv. Mater.* **2007**, *19*, 3308–3311.
- (17) Brabec, C. J.; Cravino, A.; Meissner, D.; Sariciftci, N. S.; Fromherz, T.; Rispe, M. T.; Sanchez, L.; Hummelen, J. C. *Adv. Funct. Mater.* **2001**, *11*, 374–380.
- (18) Lenes, M.; Wetzelaer, G.-J. A. H.; Kooistra, F. B.; Veenstra, S. C.; Hummelen, J. C.; Blom, P. W. M. *Adv. Mater.* **2008**, *20*, 2116–2119.
- (19) Ross, R. B.; Cardona, C. M.; Guldi, D. M.; Sankaranarayanan, S. G.; Reese, M. O.; Kopidakis, N.; Peet, J.; Walker, B.; Bazan, G. C.; Van Keuren, E.; Holloway, B. C.; Drees, M. *Nat. Mater.* **2009**, *8*, 208–212.
- (20) Lenes, M.; Shelton, S. W.; Sieval, A. B.; Kronholm, D. F.; Hummelen, J. C.; Blom, P. W. M. *Adv. Funct. Mater.* **2009**, *19*, 3002–3007.
- (21) Mikroyannidis, J. A.; Kabanakis, A. N.; Sharma, S. S.; Sharma, G. D. *Adv. Funct. Mater.* **2011**, *21*, 746–755.
- (22) Murata, M.; Morinaka, Y.; Murata, Y.; Yoshikawa, O.; Sagawa, T.; Yoshikawa, S. *Chem. Commun.* **2011**, *47*, 7335–7337.
- (23) Laird, D. W.; Stegamat, R.; Richter, H.; Vejins, V.; Scott, L.; Lada, T. A., Patent WO 2008/018931 A2.
- (24) He, Y.; Chen, H.-Y.; Hou, J.; Li, Y. *J. Am. Chem. Soc.* **2010**, *132*, 1377–1382.
- (25) Zhao, G.; He, Y.; Li, Y. *Adv. Mater.* **2010**, *22*, 4355–4358.
- (26) He, Y.; Zhao, G.; Peng, B.; Li, Y. *Adv. Funct. Mater.* **2010**, *20*, 3383–3389.
- (27) McCullough, J. J. *Acc. Chem. Res.* **1980**, *13*, 270–276.
- (28) Backer, S. A.; Sivula, K.; Kavulak, D. F.; Fréchet, J. M. J. *Chem. Mater.* **2007**, *19*, 2927–2929.
- (29) Nakamura, Y.; O-kawa, K.; Matsumoto, M.; Nishimura, J. *Tetrahedron* **2000**, *56*, 5429–5434.
- (30) Cheng, Y.-J.; Liao, M.-H.; Chang, C.-Y.; Kao, W.-S.; Wu, C.-E.; Hsu, C.-S. *Chem. Mater.* **2011**, *23*, 4056–4062.
- (31) Diederich, F.; Kessinger, R. *Acc. Chem. Res.* **1999**, *32*, 537–545.
- (32) Gadisa, A.; Svensson, M.; Andersson, M. R.; Inganäs, O. *Appl. Phys. Lett.* **2004**, *84*, 1609–1611.
- (33) Faist, M. A.; Keivanidis, P. E.; Foster, S.; Wöbkenberg, P. H.; Anthopoulos, T. D.; Bradley, D. D. C.; Durrant, J. R.; Nelson, J. J. *Polym. Sci., Part B: Polym. Phys.* **2011**, *49*, 45–51.
- (34) Mihailetchi, V. D.; Xie, H. X.; de Boer, B.; Koster, L. J. A.; Blom, P. W. M. *Adv. Funct. Mater.* **2006**, *16*, 699–708.
- (35) Blom, P. W. M.; Mihailetchi, V. D.; Koster, L. J. A.; Markov, D. E. *Adv. Mater.* **2007**, *19*, 1551–1566.